Renewable and Sustainable Energy Reviews 16 (2012) 1061–1073

Contents lists available at SciVerse ScienceDirect

Renewable and Sustainable Energy Reviews

journal homepage: www.elsevier.com/locate/rser

Solar drying of wastewater sludge: A review

Lyes Bennamoun *

Laboratoire des Composants Actifs et Matériaux, Faculté des Sciences Exactes, Sciences Naturelles et de la Vie, Université Larbi BenM'hidi, Oum El Bouaghi, Algeria

ARTICLE INFO

Article history:
Received 16 September 2011
Accepted 12 October 2011
Available online 4 November 2011

Keywords:
Solar energy
Drying kinetic
Shrinkage
Cracks
Design
Greenhouse

ABSTRACT

Drying constitutes an important process for wastewater sludge management, as it can reduce the mass and the volume of the product and consequently the cost of storage, handling and transport. During constant operating conditions, the drying kinetic of the sludge has shown mainly: a constant drying rate, one or two falling rate periods and a final short period with variations along the process of the physical properties of the product with the appearance of shrinkage and cracks phenomena. Solar drying was benefit as using free solar energy can reduce the cost of the operation. On the other hand, it plays an important role for the pathogen reduction until Environmental protection Agency (EPA) recommendations. In some studied cases, the value of 1000 CFU g^{-1} DS, which represents the EPA Class A pathogen requirement, for fecal coliform was attained. The general design of used solar dryers was constituted of: a greenhouse made with transparent material and a floor, where the product is speared in thick layers. Furthermore, fans and ventilations can be used in order to have homogeneous distribution of the air inside the greenhouse with replacement of humidified air with fresh one. Automatic or handle mix of the product was used once or for several times a day. In order to increase the performances of the drying system, other ways such as heating the floor using solar water heater, infrared lamps, using heat pumps or adding thermal energy storage systems were also tested. Covered solar drying has given better results than open solar drying. However, the origin of the wastewater sludge affects the obtained results. Alternatively, modeling drying systems was effectuated using heat and mass balances, applied for the air and the dried product. Solar drying of wastewater sludge has given satisfactory results.

Contents

1. Introduction

Water constitutes one of the keys of the socio-economic development and the human daily comfort. Consequently, the production of water increases with the population increase. Statistics confirm the non-homogeneous distribution of this important resource around the world; as the consumption of an inhabitant of Europe is estimated to 3000 m^3 per year. This quantity increases to 9985 m^3 per year for an inhabitant of the U.S.A. and decreases to 200 m^3 per year in the developing countries and attains 20 l per day in some regions such as Mali or Haiti [1]. In general manner, statistics show that 70% of water produced quantity is used for agriculture especially for the irrigation; however 30% are directed to the industry [1]. These important consumed quantities of water engender, of course, the production of wastes that, in some cases, can be noxious to the environment. The use of wastewater treatment plants (WWTP) was one of the novel developed solutions that permit to have drinkable water from wastewater; nevertheless it causes the production of sludge. In 2009, over 9.18 million tons of dry solids sludge is produced in China from WWTP [2]. This quantity was 5.36 million tons in the U.S.A. and around 2.00 million tons in Japan, in 1996 and 1993 respectively, as reported by Chen et al. [3,4]. The European commission [5] has given detailed statistics about the total production, in the last decade, of sewage sludge

* Corresponding author. Tel.: +213 32 42 39 83; fax: +213 32 42 39 83.
E-mail address: lyes_bennamoun@yahoo.ca

1364-0321/$ – see front matter © 2011 Elsevier Ltd. All rights reserved.
doi:10.1016/j.rser.2011.10.005

Nomenclature

A	area (m^2)
a	solar absorption coefficient
Cp	specific heat ($J\,kg^{-1}\,{}^{\circ}C^{-1}$)
E	evaporation rate (kg of water m^{-2} of ground h^{-1})
h	convective exchange coefficient ($W\,m^{-2}\,{}^{\circ}C^{-1}$)
Lv	latent heat of vaporization ($J\,kg^{-1}$)
M	mass (kg)
P	solar radiation or power ($W\,m^{-2}$)
R	radiative heat (W)
T	temperature (°C)
t or θ	time (s)
V	volume (m^3)
W or X	moisture content (% or $kg\,kg^{-1}$ dry basis)
w	humidity ratio (kg of water kg^{-1} of air)

Greek symbols

ρ	density ($kg\,m^{-3}$)
τ	coefficient of transmission

Subscripts

a	air
Bo	sludge
ext	external
in	air inlet
out	air outlet
s	solid
V sup	glass roof
V	glass
0	initial value

from urban wastewater (Table 1). It shows that some countries have increased considerably their produced quantities such as Greece, Hungary, Spain, France, Poland and the United Kingdom, conversely other countries have kept a constant production or decreased it, similar to Belgium, Bulgaria, Czech republic, Germany, Netherlands and Austria. Nowadays, agriculture, incineration and landfill uses constitute the major applications of sludge disposal. The European commission [5] has given more details for the most relevant producer countries. Table 2 shows that Spain, United Kingdom and Ireland are widely using more than 50% of their sewage sludge obtained from wastewater in agriculture against France, Germany, Hungary and Czech Republic which present moderate use between 28 and 47%. Until 2009, Greece and Netherlands have never incorporated their sewage sludge in agriculture. Netherlands, Austria, Belgium and Germany prefer the incineration use of their sludge with rates equal to: 73.62%, 44.31%, 41.01% and 36.20% respectively. France and United Kingdom present small values which did not exceed 18%. However, Bulgaria, Czech Republic and Hungary did not use incineration with a rate near zero. Greece uses the landfill for almost the totality of their sewage sludge with a rate around 86% as well as a rate of 100% from 2001 to 2005. The rate is more or less the third for Bulgaria, Ireland, Hungary and Poland. According to the values given by Chen et al. [3,4], U.S.A. is using 33.3% of their global sludge production in agriculture, 16.1% in incineration and 34% in landfill. However, for Japan these values are 0%, 75% and 25% respectively (Tables 3 and 4).

In all cases, drying constitutes an essential process, after application of the mechanical dewatering by centrifugation or filtration. It can reduce the water content below 5% dry solids leading to the decrease of waste mass and volume and in consequence the reduction of the cost for storage, handling and transport. On the other hand, drying sludge increases the low calorific value, transforming

Table 1
Total sewage sludge production for urban wastewater (values presented by millions of kilograms).

	2000	2001	2002	2003	2004	2005	2006	2007	2008	2009
Belgium	101	112	118	109	116	113	128	129	140	
Bulgaria	48	45	40	43	58	42	38	40	43	39
Czech Rep.	207	206	211	180	179	172	175	172	220	
Germany		2429			2261	2170	2049			
Ireland	34	38				60			88	
Greece		68	78	80	83	117	126	134	136	152
Spain	853	892	987	1012	1092	1121	1065	1153	1156	1205
France		954			1060				1087	
Hungary	102	115	117	152	184			260		
Netherlands	346	358	365	353	354	359	373	353	353	
Austria	315		323		305		255		254	
Poland	360	397	436	447	476	486	501	533	567	563
United Kingdom		1527	1544	1656	1721	1771	1809	1825	1814	1761

Source: [4].

Table 2
Agriculture use of sewage sludge from urban wastewater (in % of the total value).

	2000	2001	2002	2003	2004	2005	2006	2007	2008	2009	Mean value
Belgium		9.82	9.32	17.43	18.10	18.58	14.06	7.75	7.86		12.87
Bulgaria	0.00	0.00	0.00	0.00	0.00	0.00	31.58	15.00	25.58	35.90	10.81
Czech Rep.		74.76	75.36	10.00	17.32	16.86	19.43	27.91	25.00		33.33
Germany		31.08			27.78	41.98	29.87				32.68
Ireland	41.18	44.74				76.67					54.19
Greece		0.00	0.00	0.00	0.00	0.00	0.00	0.00	0.00	0.00	0.00
Spain	53.22	67.94	66.67	66.21	65.11	64.76	64.51	74.93	80.19	82.57	68.61
France		50.42			43.87				47.10		47.13
Hungary	26.47	22.61	25.64	19.08	22.28			56.92			28.83
Netherlands	0.00	0.00	0.00	0.00	0.00	0.00	0.00	0.00	0.00	0.00	0.00
Austria	11.75		12.07		12.46		15.29		15.75		13.46
Poland	14.17	12.34	15.37	12.98	14.08	13.58	16.17	18.39	19.75	21.85	15.87
United Kingdom		55.66	54.60	64.01	64.96	68.94					61.64

Source: [4].

Table 3
Incineration use of sewage sludge from urban wastewater (in % of the total value).

	2000	2001	2002	2003	2004	2005	2006	2007	2008	2009	Mean value
Belgium		58.93	60.17	17.43	24.14	31.86	33.59	52.71	49.29		41.01
Bulgaria	0.00	0.00	0.00	0.00	0.00	0.00	0.00	0.00	0.00	0.00	0.00
Czech Rep.		0.00	0.00	0.00	0.00	0.00	0.00	0.00	1.36		0.17
Germany		22.85			31.45	43.41	47.10				36.20
Ireland	0.00	0.00				0.00					0.00
Greece		0.00	0.00	0.00	0.00	0.00	0.00	1.49	17.65	0.00	2.13
Spain	8.21	6.17	6.99	7.61	7.05	6.96	3.85	0.00	0.00		5.20
France		17.40			16.79				18.95		17.71
Hungary	0.00	0.00	0.00	0.00	0.00			0.77			0.13
Netherlands	52.02	58.10	55.89	63.46	75.99	82.73	87.13	92.07	95.18		73.62
Austria	47.62		50.15		49.51		38.43		35.83		44.31
Poland	1.67	1.76	1.61	1.34	0.21	1.23	0.80	0.38	1.06	1.60	1.17
United Kingdom		15.78	19.82	18.96	15.86	15.92					17.27

Source: [4].

Table 4
Landfill use of sewage sludge from urban wastewater (in % of the total value).

	2000	2001	2002	2003	2004	2005	2006	2007	2008	2009	Mean value
Belgium		16.07	11.02	13.76	7.76	3.54	0.00	0.00	0.00		6.52
Bulgaria	0.00	0.00	0.00	0.00	87.93	54.76	42.11	52.50	41.86	28.21	30.74
Czech Rep.		18.45	18.96	12.78	13.97	6.98	8.00	5.23	12.27		12.08
Germany		6.59			3.49	1.24	0.24				2.89
Ireland	50.00	52.63				16.67					39.77
Greece		100.00	100.00	100.00	100.00	100.00	97.62	55.22	52.94	71.71	86.39
Spain	17.94	14.69	16.31	16.11	14.93	14.54	15.77	0.00	0.00		12.25
France		24.11			20.94				8.28		17.78
Hungary	46.08	47.83	40.17	40.13	28.80			29.62			38.77
Netherlands	18.50	17.60	10.96	4.53	4.24	3.90	4.02	0.00	0.00		7.08
Austria	13.33		11.46		9.84		9.80		8.27		10.54
Poland	42.22	50.13	44.04	36.91	34.24	31.07	29.34	23.45	16.23	14.56	32.22
United Kingdom		7.99	8.03	5.31	3.89	5.42					6.13

Source: [4].

the product into an acceptable combustible. Also, the treatment by high temperatures makes the product as pathogen free stabilized material [6–8].

The physico-chemical composition of several sewage sludges harvested from different WWTP in the world and the elements range are represented in Table 5 [3,4,9–11]. The results show the existence of important minerals that can be functional for agriculture and soil utilization and other elements that must be treated or eliminated. Moreover, the table shows difference in the element concentrations, depending on the source of the sludges.

2. Behaviour of wastewater sludge during drying

The general behaviour of the wastewater sludge during drying process, under constant operating conditions is divided by Deng et al. [2], and confirmed by Vaxelaire and Cézac [12], into 4 principal parts, as shown in Fig. 1, which represents a typical drying curve. The water removed in the first part (line AB) is considered as free water. After that, we have a succession of two falling rates; the first is represented by the line BC and the second by the curve CD. The water removed in these parts is, respectively, interstitial and surface water. The last period of the curve is a short interval, where bound water is removed and equilibrium moisture is reached. However, Deng et al. [1] observe in their experimental labour the inexistence of the constant drying rate during drying of municipal sewage sludge. They report this observation due to the utilization, before applying drying process, of the mechanical dewatering which removes all the free water. The same observation was made by Tao et al. [13] during their utilization of the mechanical dewatering of different types of wastewater sludges. The experimental work developed by Léonard et al. [7,14] has shown that the behaviour of the wastewater sludge during drying depends on the origin of the sludge, as illustrated in Fig. 2. Sludge A shows a clear constant drying rate period which is not the case of sludge B. However, the other falling periods and the short final period are observed for both sludges. Reyes et al. [15] and Léonard et al. [14] have studied the effect of the drying operating conditions, in particular the influence of the air temperature and its superficial velocity, as exposed in Fig. 3(a) and (b). The results presented in these figures point towards that drying are strongly affected by the air temperature and with a smaller degree by its superficial velocity, similar results were found for the treatment of food drying [16–19]. In general way, increasing, the temperature and the superficial velocity, lead to the increase of the drying rate. On the other hand, we observe at the beginning of the process (at the point $X = 2.6\ \mathrm{kg\,kg^{-1}}$ to around $2.4\ \mathrm{kg\,kg^{-1}}$) the existence of a very short first period caused by the adaptation of the product to the operating

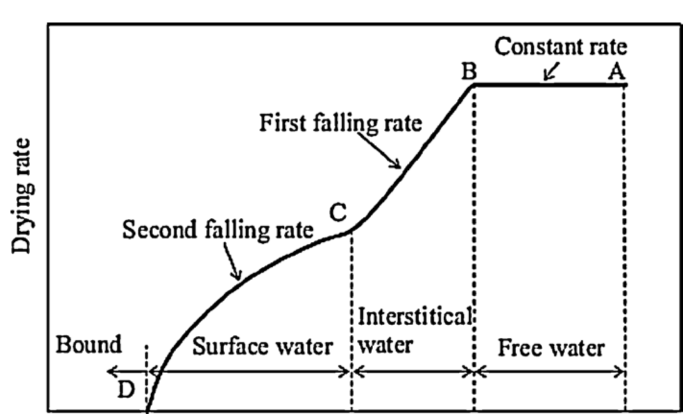

Fig. 1. Typical sludge drying curve [2].

Table 5
Physico-chemical properties of several sludges.

Parameter	Sludge A	Sludge B	Sludge C	Range
pH	7.6 ± 0.8		7.6 ± 0.1	5.0–8.0
Moisture content (%)		85.0		
Dry matter (%)			18.0 ± 0.6	
Total solids (TS, %)	20.6 ± 1.8			3.0–7.0
Volatile solids (%)	60.4 ± 2.1 (of TS)	72.9 (of dry solids DS)		60–80 (of TS)
Nitrogen (N, %)	5.38 ± 2.13		3.34 ± 0.1	1.5–5.0 (% of TS)
Phosphorus (P_2O_5, %)	2.7 ± 0.6		2710 ± 9.2 mg kg^{-1}	0.5–2.8 (% of TS)
Potash (K_2O, %)				0.0–1.0 (% of TS)
Heat value (kJ kg^{-1} dry basis DB)				18,500–30,000
Alkalinity (mg l^{-1} as $CaCO_3$)				500–1500
Arsenic (As, mg kg^{-1} DB)	44.9 ± 5.7			1.1–230
Cadmium (Cd, mg kg^{-1})	1.3 ± 0.4	1.5 (DS)	2.0 ± 0.5	1–3410 (DB)
Chromium (Cr, mg kg^{-1})	321 ± 15	26.7 (DS)	243 ± 10	10–99,000 (DB)
Copper (Cu, mg kg^{-1})	388 ± 18	154.4 (DS)	19 ± 1.0	84–17,000 (DB)
Lead (Pb, mg kg^{-1})	29.2 ± 3.6	43.3 (DS)	34 ± 2.0	13–26,000 (DB)
Mercury (Hg, mg kg^{-1} DB)				0.6–56
Molybdenum (Mo, mg kg^{-1} DB)				0.1–214
Nickel (Ni, mg kg^{-1})	128 ± 12	21 (DS)	79.0 ± 3.0	2–5300 (DB)
Selenium (Se, mg kg^{-1} DB)				1.7–17.2
Zinc (Zn, mg kg^{-1})	541 ± 73	616.3 (DS)	1435 ± 15	101–49,000 (DB)
Iron (Fe, mg kg^{-1})	10,375 ± 675	5128.6 (DS)		1000–154,000 (DB)
Cobalt (Co, mg kg^{-1} DB)				11.3–2490
Tin (Sn, mg kg^{-1} DB)				2.6–329
Manganese (Mn, mg kg^{-1})	165 ± 8	144.4 (DS)		32–9870 (DB)

Source: Sludge A: [9], Sludge B: [10], Sludge C: [11] and Range: [3,4].

conditions and represented by an increase of the drying rate. Usually, this period is neglected in modeling and simulation works [15,20,21]. Léonard et al. [6] have experimented in their work two wastewater sludges. The constant drying rate, made known in Fig. 4 by "reference", was clearly observed. One of the objectives of the work was to study the effect of the expansion of the sludge extrudates bed due to increasing additions of dry product and variations were followed using X-ray tomography. As shown in the figure, the constant drying period was made shorter with the bed expansion increase until it roughly disappearance.

3. Phenomena occurring to wastewater sludge during drying process

Léonard et al. [8,22,23], Tao et al. [13], Hsu et al. [24] and Ruiz et al. [25,26] observed the creation of two phenomena that take place inside the sludge during drying process. The phenomena are: shrinkage and cracks.

Shrinkage consists on the reduction of the product size because of the loss of its water during drying process. In spite of the importance of the phenomenon and the engendered changes in the product physical properties, it was recently introduced especially in food drying [18,27–29]. In addition, shrinkage was observed during wastewater sludge drying by Tao et al. [13] (Fig. 5). The upper images of the figure were scanned using micro-computerized tomography scanner (micro-CT) and the lower images are the 2-D

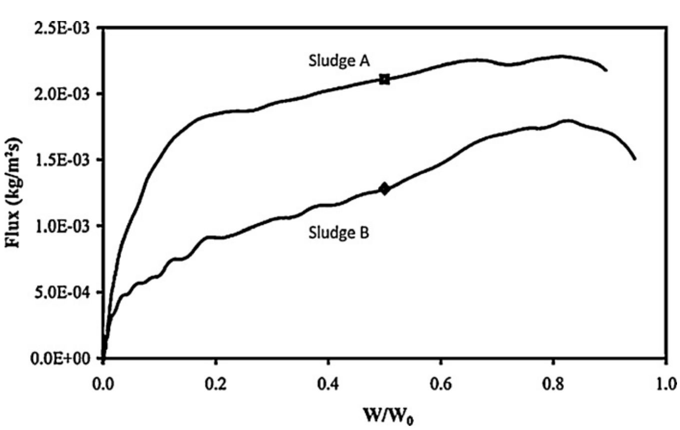

Fig. 2. Drying kinetic curve for two sludges at 160 °C, 1 m s^{-1} and 0.006 kg kg^{-1} [13].

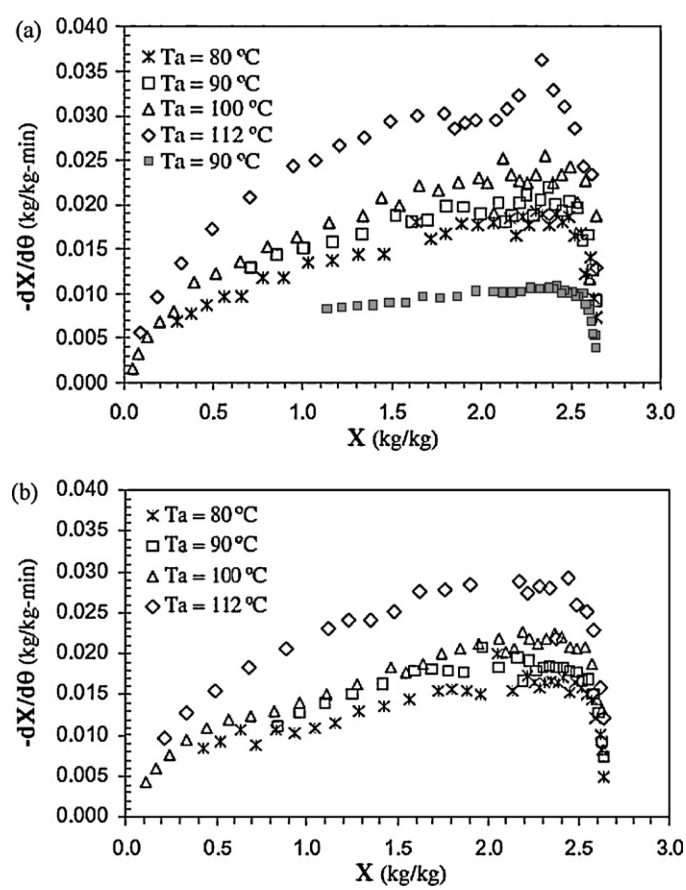

Fig. 3. Influence of the operating conditions on the behaviour of the drying kinetics [14]: (a) V_a = 0.65 m s^{-1}, (b) V_a = 0.43 m s^{-1}.

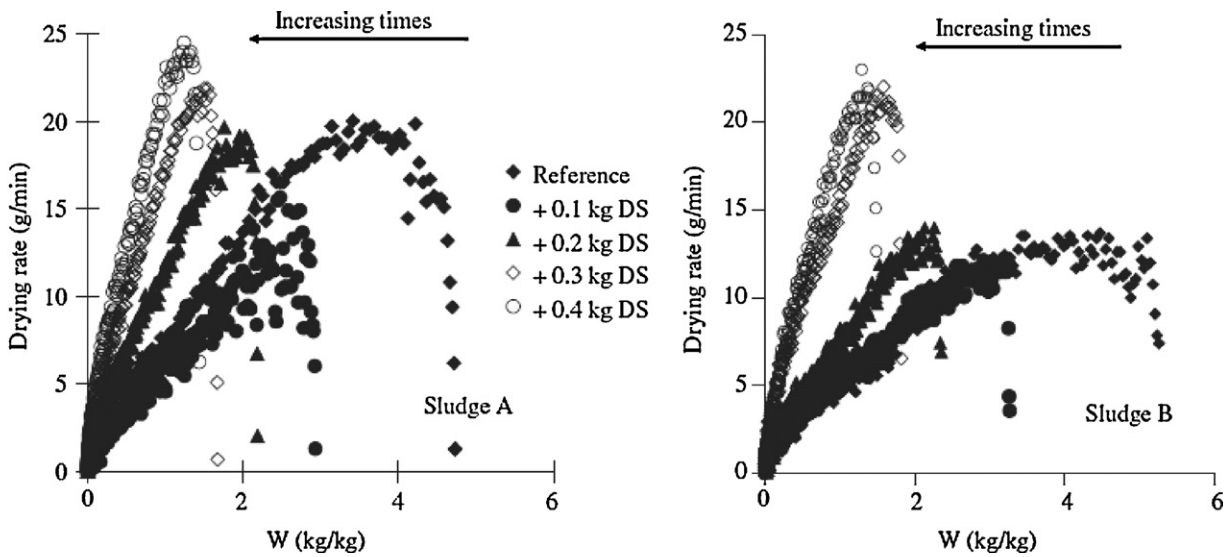

Fig. 4. Drying kinetics of two wastewater sludges with back mixing influence [5].

reconstituted transversal section of the upper images. In the same way and as shown in Fig. 6, Léonard et al. [8,22,23] follow the effect of the moisture content decrease using X-ray microtomography. The water content inside the product was calculated on the base of the variations of the grey level of water, wet and dry solid. On the other hand, the authors have observed cracks at the interior and the surface of the dried product at the same time as shrinkage happens. Shrinkage starts with the drying process begin (Fig. 7) and continue until reaching a constant value evaluated between 0.4 and 0.2 of the initial volume, depending on the origin of the

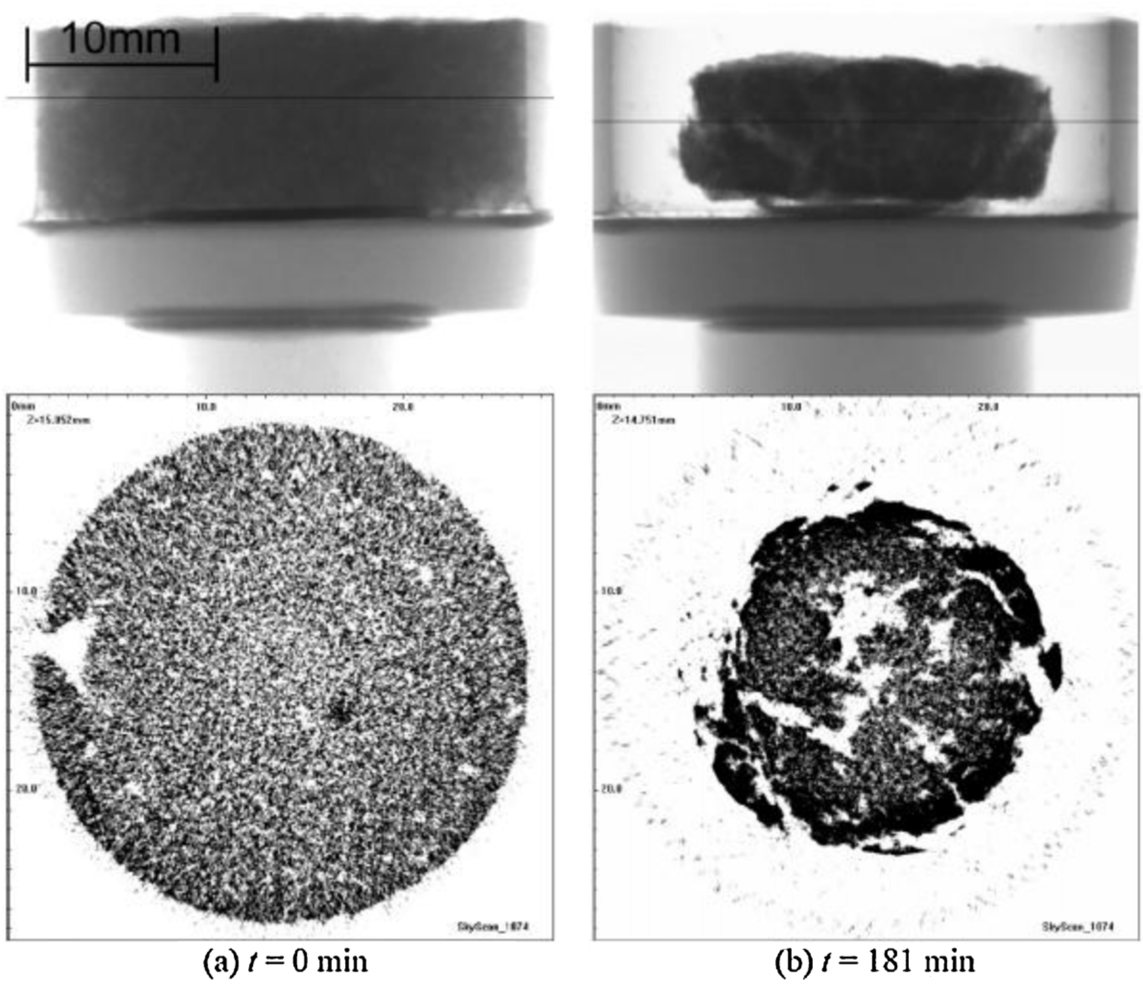

Fig. 5. Observation of shrinkage during wastewater sludge drying [13].

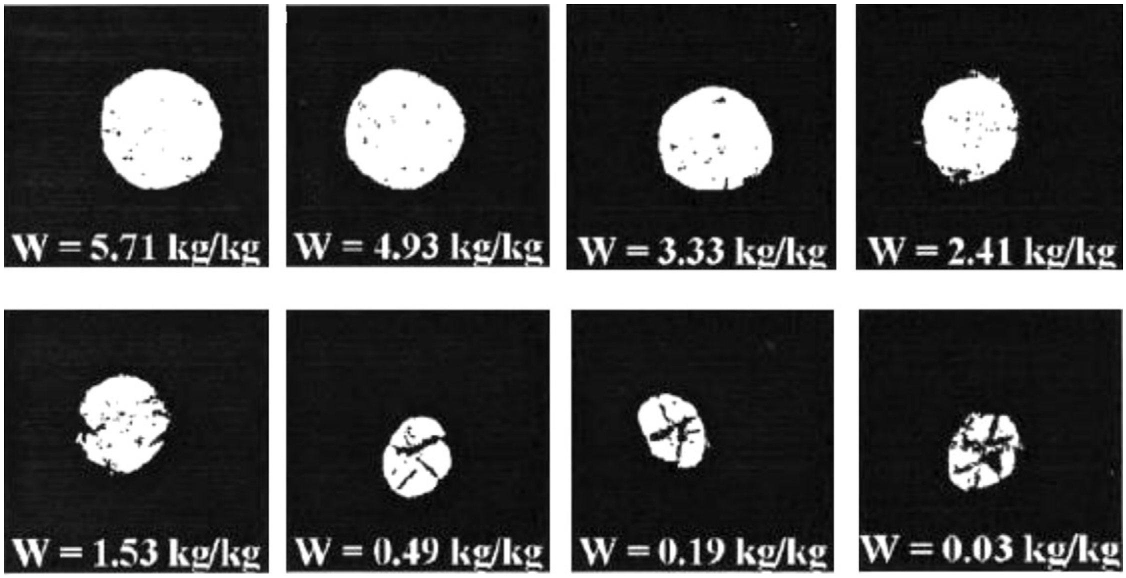

Fig. 6. 2D cross section images at different water content illustrating shrinkage and cracks development [23].

Table 6
Initial and final dimensions of extrudate samples of two different wastewater sludges [8].

	Sludge A		Sludge B	
	Extrudate 1	Extrudate 2	Extrudate 1	Extrudate 2
Initial equivalent diameter (mm)	12.74 ± 0.18	12.64 ± 0.08	13.00 ± 0.32	13.11 ± 0.12
Final equivalent diameter (mm)	7.40 ± 0.44	7.48 ± 0.39	10.09 ± 0.23	9.35 ± 0.90
Initial height (mm)	15.98 ± 0.34	15.91 ± 0.33	16.29± 0.29	16.36 ± 0.28
Final height (mm)	9.29 ± 0.20	9.04 ± 0.40	12.67 ± 0.10	12.67 ± 0.07

wastewater sludge. Table 6 gives the initial and final dimensions of the dried product. It shows an isotropic reduction varying between 77% and 58%, in both diameter and height of the product, which gives the announced precedent shrinkage rates. However, cracks show constant low values at the beginning of the process. These values increase with the moisture content decrease, until attaining values around 0.35 and more than 0.5, with an influence of the operating drying conditions, as illustrated in Fig. 8 and the origin of the sludge.

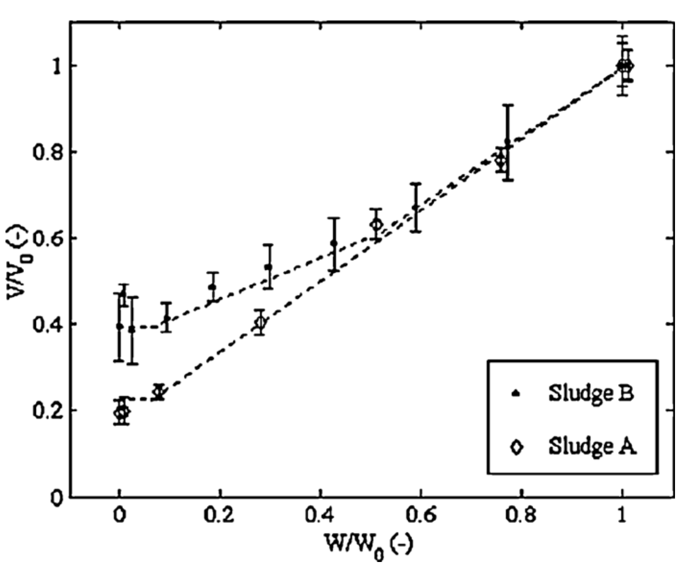

Fig. 7. Shrinkage curve for two different wastewater sludges [8].

4. Solar drying of wastewater sludge: a review

Applying free solar energy may well be an alternative solution for reduction of the cost of the drying process. However, contrary to drying with constant conditions, the obtained drying kinetics during solar drying present some variations, as the operating conditions continuously change with time. It was found that at variation of the operating conditions; the product adapts its comportment to the new conditions by varying the common direction of its drying kinetic with a non-instant adaptation and registration of a time of reaction [18,30,31].

Salihoglu et al. [9] present the performances of a solar drying plant situated in Bursa city at the southeast of the Marmara Sea in Turkey. By the end of 2006, this country has produced around 27,000 tons of dry solids per year. Wastewater sludge was obtained from a municipal plant which has a capacity of 64,000 m^3 per day. Covered and open sludge drying plants were constructed with floor dimensions of 2 m × 5 m to conduct the experiments. The two plants were operated according to the conceptual model shown in Fig. 9. For both plants, the sludge was spread out on the floors in 25 cm-layers.

The covered sludge drying plant was constructed as a tunnel type greenhouse with a roof height of 2.5 m. It was completely enclosed by two walls, 10 mm thick transparent polycarbonate sheet with light transmittance of 80%. The indoor air accumulated in the plant during the day is directed to the rock-bed for energy storage. The schematic view of the plant is shown in Fig. 10. Aeration of the surface of the sludge is effectuated by a ventilator fixed in the roof. The saturated sludge surface layer was removed with the ventilator turbulent air. Besides, saturated air by accumulation was discharged by means of two fans mounted above the doors of the plant, and air renewal was provided. The impermeable concrete

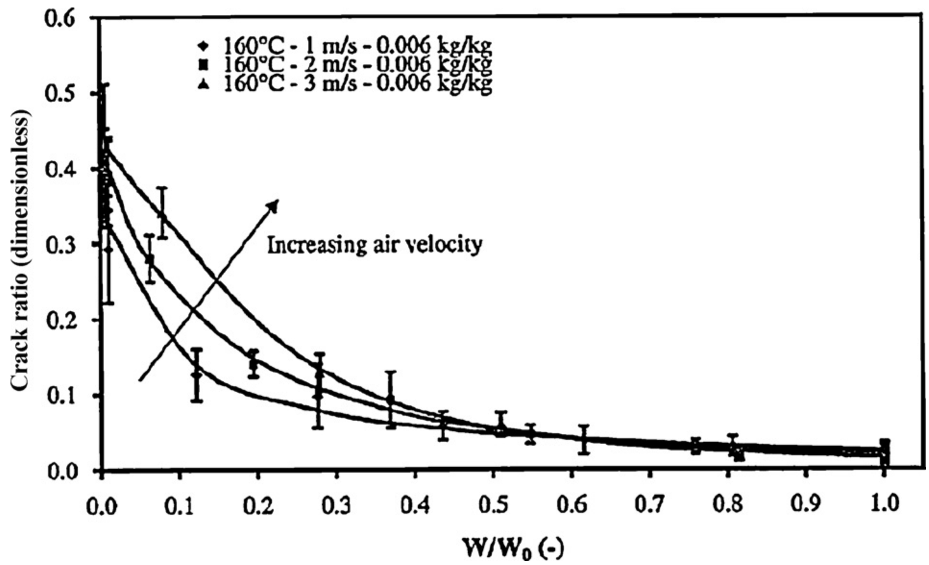

Fig. 8. Development of cracks during drying of wastewater sludge [23].

floor of the greenhouse was heated using hot water pipes connected to two flat plate solar collectors. Under the concrete floor, a rock-bed, composed of 16–48 mm diameter stones and 50 cm depth, is used as storage system. The bottom and sidewalls of the rock-bed were insulated with an impermeable concrete floor and heat insulation material. Every day and for two times, the sludge was mixed manually for sludge renewal purposes.

On the other hand, an impermeable concrete floor is constructed for the open sludge drying plant. Surface aeration was supplied with the wind effect and sludge was heated with direct exposure to the sun. Also, the sludge was mixed manually twice a day.

As commented before regarding the adaptation of the drying kinetic its behaviour during application of variable conditions, Fig. 11 show the total dependence of the moisture content variations on the climatic conditions with a non-regular decrease, in particular sludge dried in the open plant. In this plant and after 55 days of drying time the moisture content was around 60%. However, it has reached 20%, for the same time, for a sludge dried in the covered plant. With lime added the performances of both plants were ameliorated and the total amount of the sludge to be disposed would be reduced by approximately 40%. The financial evaluation of the covered drying system gave a self amortization in only 4 years.

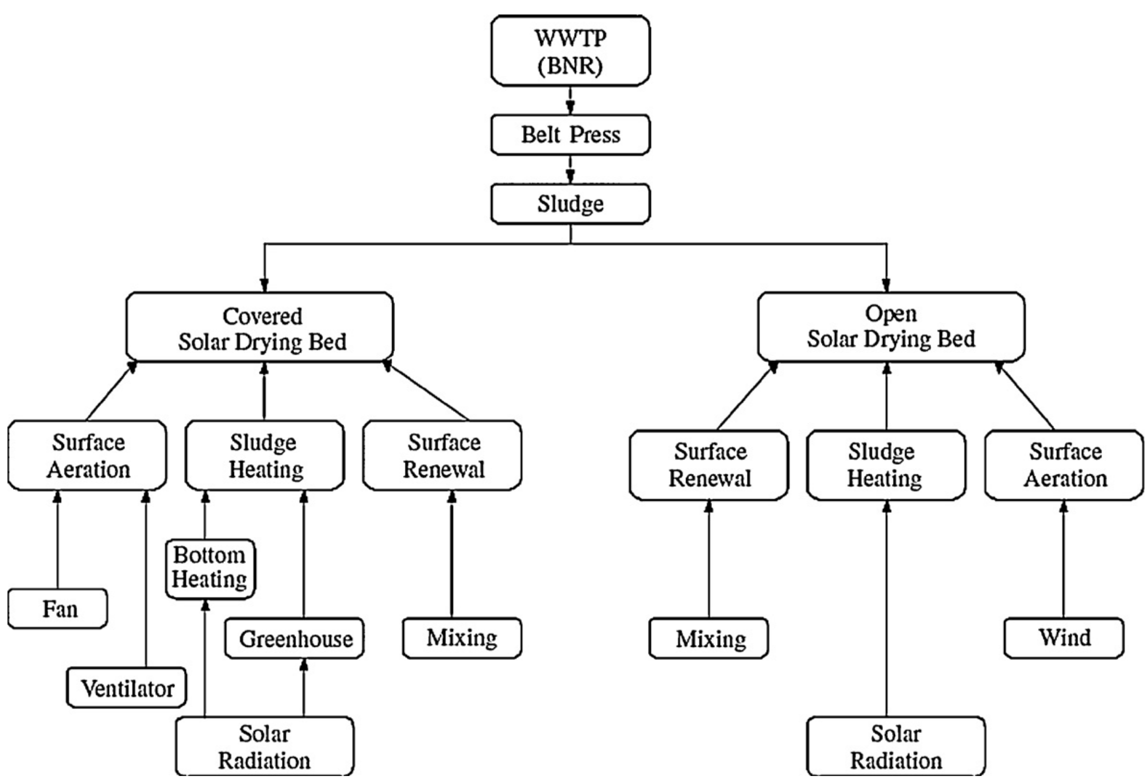

Fig. 9. Conceptual model for the experimental design [9].

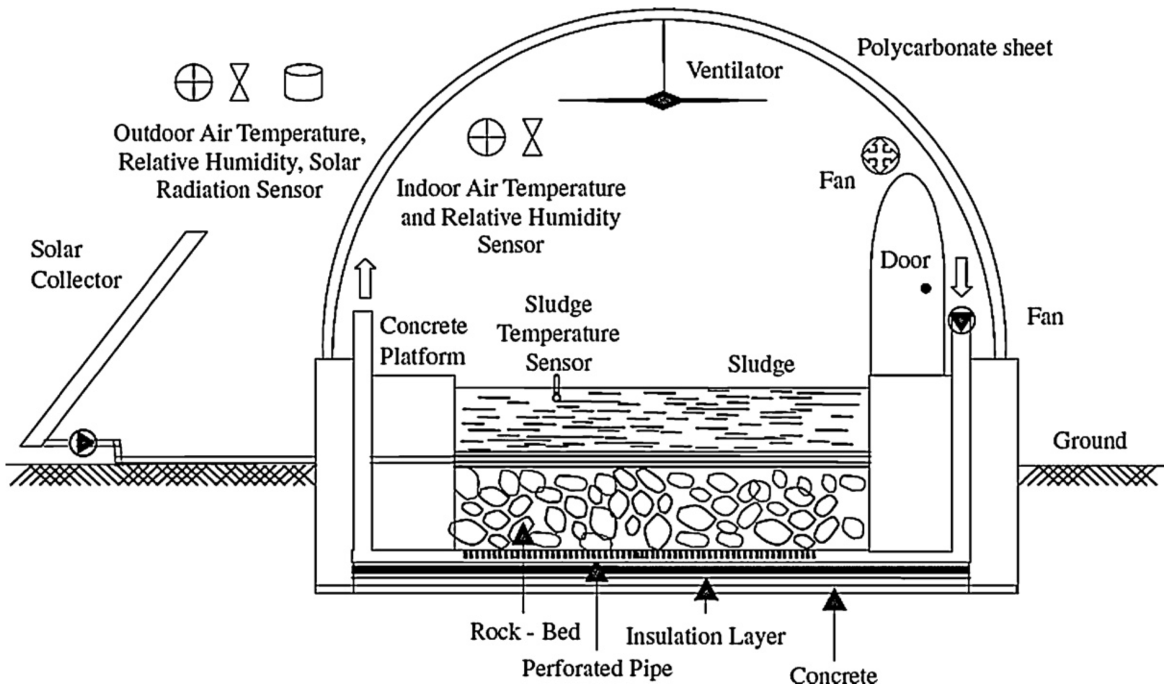

Fig. 10. Schematic view of the covered solar drying plant [9].

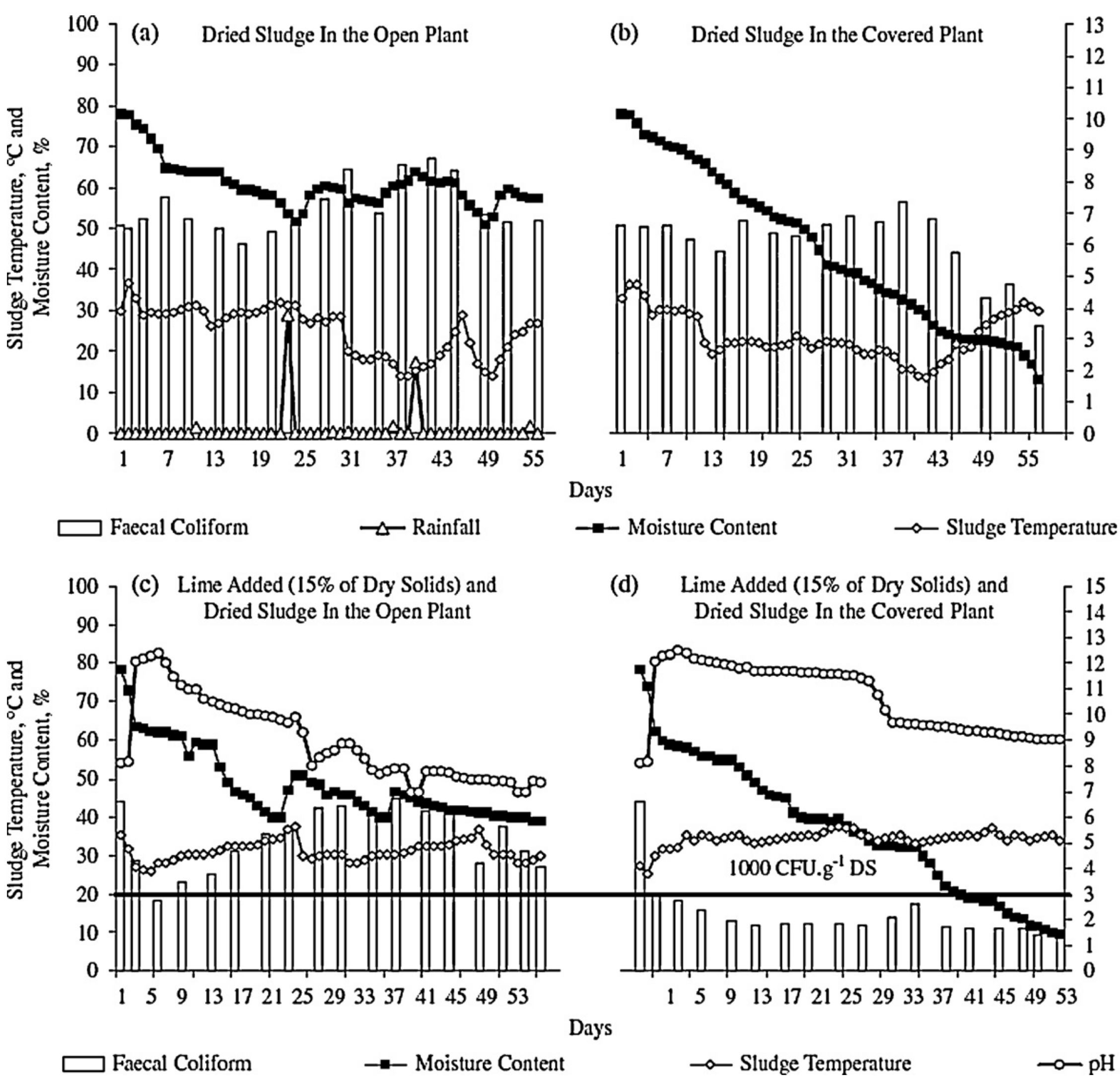

Fig. 11. Covered and open sun wastewater sludge drying in summer period [9].

Concerning the pathogen removal, a greater reduction was obtained within the covered sludge drying system comparing to the open system. Fig. 11 shows the fecal coliform reduction obtained during the solar drying in the cover and open plants, in summer period. The coliform content of the mechanically dewatered sludge was 10^7 before starting drying process. At the end of 45 days and at the application of the covered solar drying, the coliform content decreased to below 2×10^6 CFU g^{-1} DS in summer. This is the limit value of the Environmental Protection Agency (EPA) Class B pathogen requirement. However, to obtain the EPA class A pathogen requirement of 1000 CFU g^{-1} DS in a shorter time; a limited amount of lime was added to the dewatered sludge before solar drying. An average time of 10 days in summer and 20 days in winter were needed.

Lei et al. [32] developed a laboratory greenhouse, shown in Fig. 12. The greenhouse is made of glass. Its inner bottom side is painted in black in order to increase absorption of solar energy radiations. A chimney of 180 cm high was placed on the top of the greenhouse. Also, 6 air vents were made on the two walls of the greenhouse. The drying system was tested in the region of Shanghai in china. It is characterized by a maximum irradiance of 1002 W m^{-2} in summer. It decreases to 947 W m^{-2} in autumn and in spring and it decreases until 910 W m^{-2} in winter. Samples of fresh sludge were obtained from WWTP situated in Shanghai. The sludge has initial moisture of 5.16 kg kg^{-1} dry basis and was dried to 0.78 kg kg^{-1} dry basis. It was putted in 25 mm thick layers in a plate which was made of 0.1 mm steel mesh and had an area of 0.22 m × 0.36 m. The drying process has taken 125 h in summer and around 550 h in winter with a non-regular decrease of the moisture content, as illustrated in Fig. 13(a) and (b).

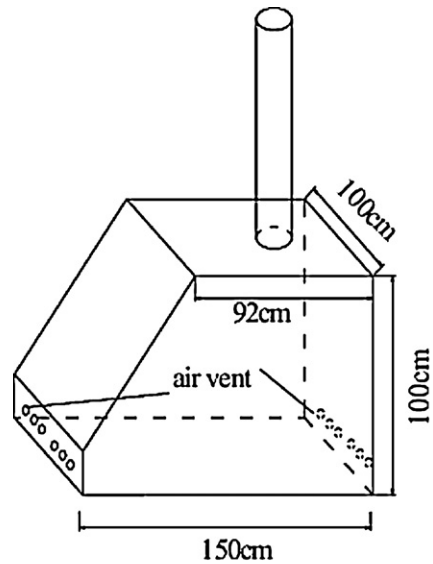

Fig. 12. Greenhouse used for sludge drying [32].

Mathioudakis et al. [10] propose drying wastewater sludge using two solar drying plants. The sludge was obtained from WWTP

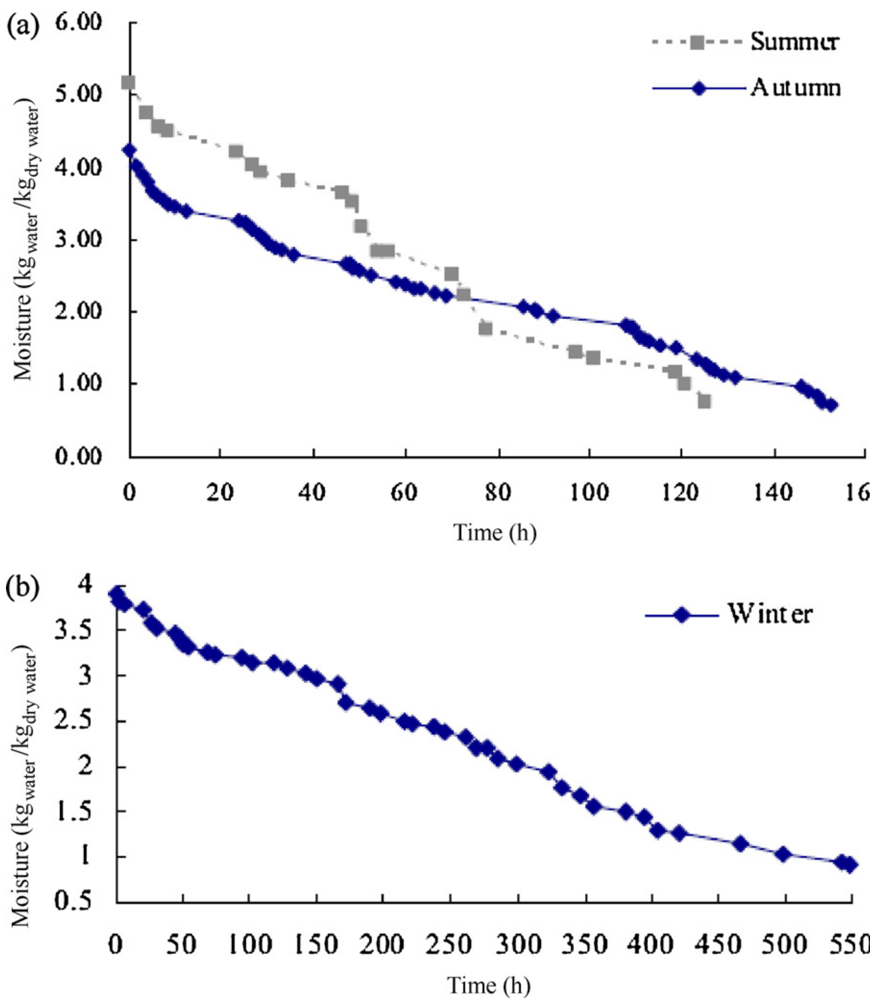

Fig. 13. Variations of the moisture content vs. time of the sludge for different seasons [32].

Fig. 14. Solar drying plants (left) and plant indoor view (right) [10].

of Komotini in Greece. Several batches of sludge were sampled after thickening and dewatering. The dewatered sludge was dried using two pilot-scale solar drying plants of approximate 2.5 m^3 each and made of polycarbonate, as it is illustrated in Fig. 14. The first plant was equipped with gravel floor, where hot water, generated by a commercial solar water heater, circulated. It permits the utilization of solar energy additionally to the energy given by the greenhouse. Hot water circulation was controlled by a thermostat, and it was performed only when the water temperature was higher than the plant indoor temperature. A fan was installed inside both plants to provide turbulent air able to remove the moisture from the surface layer. Also, two axial fans were replacing saturated air with fresh ambient air. Approximately, 8 kg of dewatered sludge were placed into crates forming a depth between 20 and 25 cm. The sludge was mixed manually once per day. The results show that the moisture content of wastewater sludge has decreased from 85% to 6% wet basis within 7–12 days in summer and to 10% as final moisture content within 9–33 days in autumn. Incorporating a solar water heater, with recirculation through the bottom of the plant has accelerated drying process by 1–9 days during winter conditions.

Before drying, the total and fecal coliform of the dewatered sludge was respectively 4×10^6 CFU g^{-1} DS and 3×10^5 CFU g^{-1} DS in summer and in autumn. After application of solar drying, the dry sludge has attained, in summer, the following values: 2×10^4 CFU g^{-1} DS as total coliform and 10^3 CFU g^{-1} DS as fecal coliform. These values were respectively 2×10^6 CFU g^{-1} DS and 8×10^5 CFU g^{-1} DS in autumn.

Slim et al. [33] have modeled a wastewater sludge drying system using climatic conditions of the region of Agen in France. Sludge is uniformly spread over a concrete floor of the greenhouse dryer. The drying system is composed of three main parts: the greenhouse, the sludge mixing engine and the heat pumps with corresponding heat sources and sinks (Fig. 15). The greenhouse is consists of a hall of 4.6 m width and 20 m length completely covered by a transparent shell, resistant to unfavourable climatic conditions. It limits loosing and exchanging heat with external air. The roof of the greenhouse has a height of 4 m under gutter and 5 m at the top. Inside the greenhouse, two walls of 0.45 m height are dividing the space of the house. The ventilation ducts are fixed on these walls to make a lateral sweeping of the house. Its floor is made of three layers: deepest one is composed of polystyrene to reduce the heat looses towards the ground. The second layer consists of a network of polyethylene tubes fixed to the polystyrene panels. The tubes are installed to ensure a uniform flux distribution inside the greenhouse. The last layer is made of 10 cm thick of concrete. Sludge is mixed inside the greenhouse using a mixing engine that operate every 12 h and prevent the formation of crusts. Two heat pumps are used in the drying system, one for heating the air and the second for heating the floor of the greenhouse. The heat pumps are controlled by an on–off strategy and its functioning depends on the climatic conditions. The authors have modeled and compared the efficiencies of the drying systems in different seasons. The modeling work was based on mass, energy and momentum laws as well as some heat transfer correlations. It was deduced that more detailed economical calculations are needed to confirm the obtained results and thus the use of the proposed model by the designers.

Roux et al. [34] tested and modeled solar drying of wastewater sludge using a greenhouse situated in the region of Fonsorbes in France. The drying unit is made up of two drying bays and is about 50 m long, 4 m height and 15 m wide. According to the design

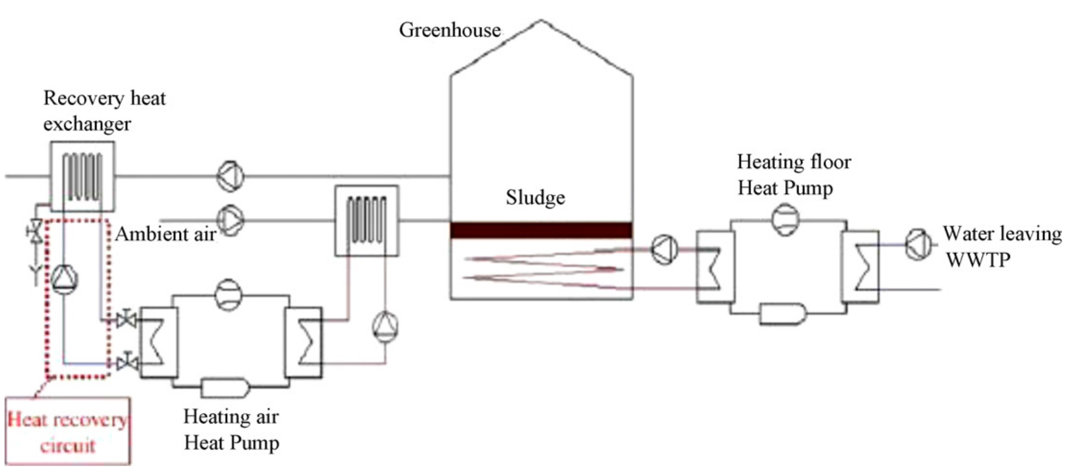

Fig. 15. Schematic diagram of the solar and heat pump sludge drying system [33].

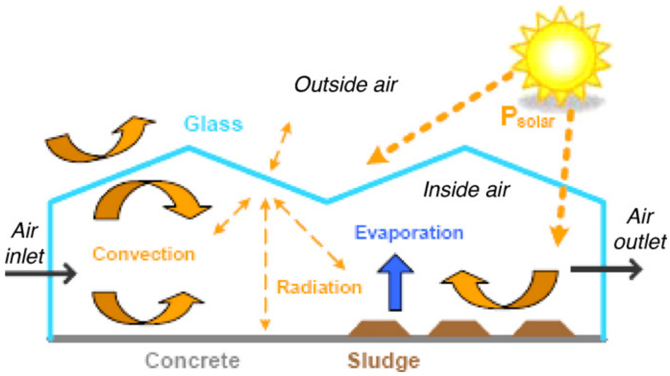

Fig. 16. Transfer phenomena in the solar drying unit [34].

geometry, shown in Fig. 16, and the operating conditions, sludge is spread only in the first bay of the green house. The design of the unit contains windrows in order to offer an optimized transfer area with the forced air flux. This high forced air renewal allows water evaporation from the sludge and the transport of the water out of the unit. Fans were placed inside the unit for ensuring homogeneous water concentration and sufficient connective transfers with the sludge. Also, a robot regularly adds some fresh sludge within windrows and mixes them to homogenize dryness and temperature.

Modeling of the drying unit passes through the establishment of heat and mass balances. So, two differential equations were obtained:

The boundary walls balances take into account solar effects, internal and external convections and infrared radiations. The differential equation of the roof of the greenhouse is written:

$$\rho_{V\,\sup} V_{V\,\sup} Cp_{V\,\sup} \frac{dT_{V\,\sup}}{dt} = [P_{V\,\sup} a_{V\,\sup} + h_{V\,\sup}(T_a - T_{V\,\sup}) + h_{ext}(T_{ext} - T_{V\,\sup})]A_{V\,\sup} + \sum_{j\,walls \neq V\,\sup} R_{j-V\,\sup} \quad (1)$$

The second differential equation is written in the following form:

$$\rho_{Bo} V_{Bo} Cp_{Bo} \frac{dT_{Bo}}{dt} = [P_{Bo} a_{Bo} \tau_V + h_{Bo}(T_a - T_{Bo})]A_{Bo} + \sum_{j\,walls \neq Bo} R_{j-Bo} + M_s L_v \frac{dX}{dt} \quad (2)$$

Experimental data are used for determination of the thin layer drying of wastewater sludge.

The modeling work has successfully permitted to follow the variations of the windrow height and the dryness evolution with time. Also, it was possible to calculate the temperature inside the greenhouse.

Krawczyk and Badyda [35] constructed and tested a pilot wastewater sludge dryer in Kamienna region in Poland. The main part of the dryer is a light steel structure covered with polycarbonate plates built on a concrete plate. The structure was fitted with ventilation system in order to provide a uniform distribution of the air over the surface of the dried sludge through a number of blowers. Also, a sludge shuffling system was installed. The solar drying system has an average daily drying rate of 8.12 kg H_2O/m^2 d. In order to increase the performances of the drying system, an auxiliary source is added. The first experienced auxiliary source was infrared (IR) lamps which gave a supplement of power assumed equal to 150 W m^{-2}. The average daily drying rate has enhanced to 11.11 kg H_2O/m^2 d. The calculus of the usage efficiency gave a rate of 57.7%. For the second investigation and in addition to solar drying, floor was heated. The average daily drying rate has attained 11.71 kg H_2O/m^2 d, with an average power output of the floor heating system equal to 225 W m^{-2} and the usage efficiency were 46.2%. The variations of the drying rate for the three proposed methods are shown in Fig. 17. It is clear that the obtained periods at application of constant operating conditions are non observable. The authors modeled the functioning of the drying system based on heat and mass transport within the dried matter, the ambient air and the border between the two areas, and using the unsteady case. The efficiency of the drying system was calculated using the following equation:

$$\eta = \frac{\Delta W \cdot r}{P \cdot 86,400} \quad (3)$$

where ΔW is, for the first studied case, the increase in the daily drying rate when using IR lamps, referenced to purely solar drying and the increase in the daily drying rate using floor heating system referenced to purely solar drying for the second case.

P is the assumed power output of the IR heating for the first case and for the second case is the average power output of the floor heating system.

The study must be completed by an economical study to know the real performances of the proposed drying systems with

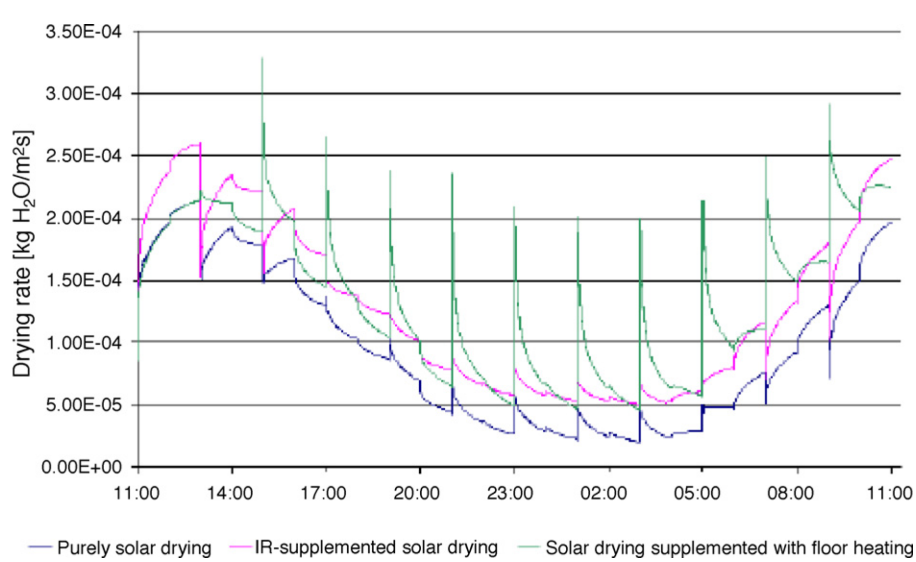

Fig. 17. Comparison of drying rate curve for purely solar drying and after adding an auxiliary source of energy [35].

supplementary heating sources. Also, in some cases, question of practicality must be treated.

Seginer et al. [36] have used one of the drying chambers existing in Füssen in Germany. The drying chamber has a concrete floor with 10 m wide and 50 m long from the wall with air inlet to the outlet wall, where fans are located. The installed capacity of the mixing fans and the ventilation fans is 150 m^3 of air per m^2 of floor and per hour. In the experiments the mixing fans can give two rates: 0 and 150 $m^3\,m^{-2}\,h^{-1}$, however the ventilation fans were operated at several rates of 30, 100 and 140 $m^3\,m^{-2}\,h^{-1}$. The fans were continuously operated at the designated rates. The sludge was mixed by a robot, on a constant daily schedule, for 4 or 6 h per day. Two methods were used to measure the loss of water; sludge sampling and vapour balance. The first method consists on the determination of the amount of the solids from the volume, bulk density and dry solids content (DSC) of the sludge. On the other hand, sampling the sludge every few days to determine its DSC is effectuated. The second measuring method consists of measuring the humidity ratio of the ventilating air at inlet and outlet then multiplying the humidity difference by the density of the air and the nominal volumetric discharge of the ventilation fans Q_v. The obtained evaporation rate is expressed:

$$E = \rho(w_{out} - w_{in}) \tag{4}$$

Four types of prediction models were considered: physical, additive, multiplicative and neural network model, the multiplicative model has shown best results. The most important predictors of evaporation rate for the conditions under consideration were solar radiation, outdoor temperature, ventilation rate and dry solids content of the sludge.

5. Conclusion

Drying is an essential process during the wastewater management, as it reduces the quantity of sludge that could be manipulated. Drying kinetic is one of the important parameters that must be known to have a better understand and control of the process. The general behaviour of the drying kinetic during wastewater sludge drying contains a short adaptation period to the applied drying conditions. Depending on the origin of the sludge, a first principle period known as a constant drying rate period can be observed. This period is generally followed by one or two falling rate periods then a short final period where bound water is removed. During all the process the product has shown shrinkage and cracks phenomena.

Using free solar energy for wastewater sludge drying can be benefit in point of view of energy consumption and in consequence on the cost of the drying system. This review has shown that in whole presented cases, the wastewater sludge is spread in thick layers, in the floor of a greenhouse chamber, which is the main part of the presented drying systems. Fans and ventilations can be added, in order to have homogeneous distribution of the inlet air at the surface layers of the product. Also, ventilation is used to evacuate the saturated air and replace it by fresh air. Generally mixing the product manually or using a robot, once or several times in a day was effectuated which permits to have harmonized distribution of the dried product. Several, materials were added in order to increase the efficiency of the drying systems, such as heat pump, infrared lamps, heating the floor of the greenhouse using solar water heater or adding rock-bed as thermal energy storage system. According to the obtained results and the cost of the operation, it was not benefit, in all cases, to use a second source of energy beside to free solar energy. The performances of the drying systems change through the period of use, the geographical situation of the place where the experimental work was done, what is more it depends on the origin of the wastewater sludge.

Several works have modeled solar drying of the wastewater sludge. It passes commonly through the establishment of heat and mass transfer applied for the air and the product with taking in consideration the variations of the solar radiations, inlet and outlet temperatures and added materials such as fans, ventilation, auxiliary sources and storage systems when they are used.

It was confirmed that using solar drying plays an interesting role for the pathogen reduction of the wastewater sludge [9–11,37]. The fecal coliform content decreases until EPA Class B pathogen requirement and even EPA Class A pathogen requirement, in some cases, such as at the use of a limited amount of lime.

For the most realized drying systems exhaustive modeling studies are needed for having more details about air and product temperature and humidity, which should give necessary information for an accurate design of solar drying of wastewater sludge system. Also, economical studies concerning the different used methods are required for calculation of the cost of the used systems and their investment feedback.

References

[1] Wikipedia, http://fr.wikipedia.org/wiki/Eau.
[2] Deng WY, Yan JH, Li XD, Wang F, Lu SY, Chi Y, et al. Measurement and simulation of the contact drying of sewage sludge in a Nara-type paddle dryer. Chemical Engineering Science 2009;64:5117–24.
[3] Chen G, Yue PL, Mujumdar AS. Dewatering and drying of wastewater treatment sludge. In: Mujumdar AS, editor. Handbook of industrial drying. CRC Press; 2006 [chapter 38].
[4] Chen G, Yue PL, Mujumdar AS. Sludge dewatering and drying. Drying Technology 2002;20:883–916.
[5] Eurostat de la commission Européenne du 19 Mars 2010, http://epp.eurostat.ec.europa.eu/portal/page/portal/product_results/search_results?mo=containsall&ms=boue&saa=&p_action=SUBMIT&l=f&co=equal&ci=&po=equal&pi=.
[6] Léonard A, Meneses E, Le Trong E, Salmon T, Marchot P, Toye D, et al. Influence of back mixing on the convective drying of residual sludges in a fixed bed. Drying Technology 2008;42:2671–7.
[7] Léonard A, Vandevenne P, Salmon T, Marchot P, Crine M. Wastewater sludge convective drying: influence of sludge origin. Environmental Technology 2004;25:1051–7.
[8] Léonard A, Blacher S, Pirard R, Marchot P, Pirard JP, Crine M. Multiscale texture characterization of wastewater sludges dried in a convective rig. Drying Technology 2003;21:1507–26.
[9] Salihoglu NK, Pinarli V, Salihoglu G. Solar drying in sludge management in Turkey. Renewable Energy 2007;32:1661–75.
[10] Mathioudakis VL, Kapagiannidis AG, Athanasoulia E, Diamantis VI. Extended dewatering of sewage sludge in solar drying plants. Desalination 2009;248:733–9.
[11] Öğleni N, Özdemir S. Pathogen reduction effects of solar drying and soil application in sewage sludge. Turkish Journal of Agriculture and Forestry 2010;34:509–15.
[12] Vaxelaire J, Cézac P. Moisture distribution in activated sludges: a review. Water Research 2004;38:2215–30.
[13] Tao T, Peng XF, Lee DJ. Thermal drying of wastewater sludge: change in drying area owing to volume shrinkage and crack development. Drying Technology 2005;23:669–82.
[14] Léonard A, Blacher S, Marchot P, Pirard JP, Crine M. Convective drying of wastewater sludges: influence of air temperature, superficial velocity and humidity on the kinetics. Drying Technology 2005;23:1667–79.
[15] Reyes A, Eckholt M, Troncoso F, Efremov G. Drying kinetics of sludge from a wastewater treatment plant. Drying Technology 2004;22:2135–50.
[16] Toğrul IT, Pehlivan D. Modeling of drying kinetics of single apricot. Journal of Food Engineering 2003;58:23–32.
[17] Azzouz S, Guizani A, Jomaa W, Belghith A. Moisture diffusivity and drying kinetic equation of convective drying of grapes. Journal of Food Engineering 2002;55:323–30.
[18] Bennamoun L, Belhamri A. Numerical simulation of drying under variable external conditions: application to solar drying of seedless grapes. Journal of Food Engineering 2006;76:179–87.
[19] Bennamoun L, Belhamri A. Study of heat and mass transfer in porous media: application to packed-bed drying. Fluid Dynamics and Materials Processing 2008;4:221–30.
[20] Bennamoun L, Léonard A. Etude expérimentale et modélisation du séchage de boues générées par l'épuration des eaux usées. Revue des Énergies Renouvelables 2011;14:1–12.

[21] Bennamoun L, Belhamri A, Léonard A. Contribution to the modeling of wastewater sludge drying kinetics: study of the operating conditions effect. In: Mujumdar AS, editor. Drying 2010. 2010. p. 828–33.
[22] Léonard A, Blacher S, Marchot P, Pirard JP, Crine M. Moisture profiles determination during convective drying using X-ray microtomography. The Canadian Journal of Chemical Engineering 2005;83:127–31.
[23] Léonard A, Blacher S, Marchot P, Pirard JP, Crine M. Measurement of shrinkage and cracks associated to convective drying of soft materials by X-ray microtomography. Drying Technology 2004;22:1695–708.
[24] Hsu JP, Tao T, Su A, Mujumdar AS, Lee DJ. Model for sludge cake drying accounting for developing cracks. Drying Technology 2010;28:922–6.
[25] Ruiz T, Wisniewski C, Kaosol T, Persin F. Influence of organic content in dewatering and shrinkage of urban residual sludge under controlled atmospheric drying. Transactions of IChemE Part B: Process Safety and Environmental Protection 2007;85:104–10.
[26] Ruiz T, Wisniewski C. Correlation between dewatering and hydro-textural characteristics of sewage sludge during drying. Separation and Purification Technology 2008;61:204–10.
[27] Bennamoun L, Belhamri A. Mathematical description of heat and mass transfer during deep bed drying: effect of product shrinkage on bed porosity. Applied Thermal Engineering 2008;28:2236–44.
[28] Ramos IN, Brandão TRS, Silva CLM. Integrated approach on solar drying, pilot convective drying and microstructural changes. Journal of Food Engineering 2005;67:195–203.
[29] Simal S, Rosselló C, Mulet A. Drying of shrinking cylinder-shaped bodies. Journal of Food Engineering 1998;37:423–35.
[30] Bennamoun L, Belhamri A, Ali-Mohamed A. Application of a diffusion model to predict drying kinetics changes under variable conditions: experimental and simulation study. Fluid Dynamics and Materials Processing 2009;5:177–91.
[31] Kooli S, Fadhel A, Farhat A, Belghith A. Drying of red pepper in open sun and green house conditions. Mathematical modeling and experimental validation. Journal of Food Engineering 2007;79:1094–103.
[32] Lei Z, Dezhen C, Jinlong X. Sewage sludge solar drying practise and characteristics study. In: Proceedings of power engineering conference, IEEE. 2009.
[33] Slim R, Zoughaib A, Clodic D. Modeling of a solar and heat pump sludge drying system. International Journal of Refrigeration 2008;31:1156–68.
[34] Roux N, Jung D, Pannejon J, Lemoine C. Modelling of the solar drying process Solia. In: Pierucci S, Ferraris GB, editors. Proceeding of 20th European symposium on computer aided process engineering. 2010.
[35] Krawczyk P, Badyda K. Modeling of thermal and flow processes in a solar wastewater sludge dryer with supplementary heat supply from external sources. Journal of Power Technologies 2011;91:37–40.
[36] Seginer I, Bux M. Modeling solar drying rate of wastewater sludge. Drying Technology 2006;24:1353–63.
[37] Albino DS, Barros PR, da Rocha Neto JS, van Haandel AC, Caviacanti PF. Modelling and estimation of physical parameters in a sludge drying system. Water Science and Technology 2002;45:389–96.